Proton NMR Study on Selective Hydration of Anions in Nitrobenzene

Toshiyuki Osakai,*,† Motohiko Hoshino,† Mariko Izumi,† Masaru Kawakami,‡ and Kazuyuki Akasaka‡

Department of Chemistry, Faculty of Science, Kobe University, Nada, Kobe 657-8501, Japan, and Department of Molecular Science, Graduate School of Science and Technology, Kobe University, Nada, Kobe 657-8501, Japan

The selective hydration of univalent anions ($X^- = Cl^-$, Br^-, I^-, NO_3^-, ClO_4^-, SCN^-) in deuterated nitrobenzene was studied by means of ^1H NMR spectroscopy. The dependence of the chemical shift of water protons upon water- and ion-concentrations clearly showed that the selective hydration to the anions can be elucidated in terms of the successive reaction mechanism: $X^-(H_2O)_{m-1} + H_2O \rightleftharpoons X^-(H_2O)_m$ ($m = 1, 2, 3, ...$). By curve-fitting analyses, the successive formation constants and the intrinsic chemical shifts could be evaluated for the hydrated anions in different hydration states. Spin−lattice relaxation times were also measured for various water- and ion-concentrations, and likewise analyzed on the basis of the successive reaction mechanism. The intrinsic rotational correlation times evaluated for the hydrated anions in different states were usually larger than ∼3 ps for free waters, suggesting the restriction of the rotational diffusion of water molecules by bonding with the anions.

Introduction

Previous solvent extraction studies[1−10] have shown that water molecules are co-extracted into water-immiscible organic solvents with hydrophilic ions such as Li^+, Na^+, Ca^{2+}, Ba^{2+}, Cl^-, and Br^-. Even a water-immiscible solvent such as nitrobenzene (NB) usually dissolves a considerable amount of water (e.g., 0.168 M H_2O in NB;[10] M = mol dm^{-3}). Accordingly, such phenomena can be elucidated in terms of selective solvation of ions in mixed solvents.[11] This is a key concept intimately related to various ion-transfer processes in separation- and detection-systems including solvent extraction, membrane transport, and ion-selective electrodes. Also, it has a fundamental significance for understanding a role of water in biological systems. For instance, a significant role of water molecules in hydrophobic cores in proteins has been recognized (e.g., a light-driven proton pump, bacteriorhodopsin[12]).

In a recent theoretical study[13] on the transfer of hydrated ions across the organic solvent (O)/water (W) interface. Osakai and Ebina have proposed a new, non-Bornian theory of the Gibbs free energy ($\Delta G_{tr}^{o,O \to W}$) of ion transfer across the O/W interface. The theory is based on short-range ion−solvent interactions, in which a hydrophilic ion such as Na^+ and Cl^- is assumed to transfer to the O-phase as the hydrated ion. A similar assumption was made by Sánchez et al.[14] who calculated $\Delta G_{tr}^{o,O \to W}$ for several hydrophilic ions using a Born-type electrostatic solvation model. Such an assumption for hydrated-ion transfer appears to be supported by molecular dynamics computer simulations.[15,16] Volkov and co-workers[17,18] also suggested that hydrated rather than bare ions should permeate through lipid bilayers.

Experimentally, the selective hydration of ions in water-miscible or -immiscible solvents has been studied by solubil-ity,[19,20] polarography,[21] UV−visible,[22,23] ^1H NMR,[2,20,23−25] IR,[25−27] and other methods[20,28] (also see ref 11). Among these methods, NMR[29] is one of the most powerful techniques. In 1972, Kawasaki et al.[2] applied ^1H NMR to the calcium ion in water-immiscible NB, and observed changes in a chemical shift of water as a function of the water content. Ito et al.[23] measured the chemical shift of water protons for the iodide ion in NB, and found that the low-field shift of water protons with water- and ion-concentrations can be explained in terms of the successive reaction mechanism, $I^- \rightleftharpoons I^-(H_2O) \rightleftharpoons I^-(H_2O)_2 \rightleftharpoons I^-(H_2O)_3$. While this mechanism is very likely, the further verification of the mechanism seems to be needed.

In the present study, we have utilized ^1H NMR spectroscopy at 400 MHz to study the selective hydration phenomena for typical univalent anions ($X^- = Cl^-$, Br^-, I^-, NO_3^-, ClO_4^-, SCN^-) in deuterated nitrobenzene (NB-d$_5$). For the respective anions, dependences of the chemical shift of water upon water- and ion-concentrations have been examined. We have found that the selective hydration of these anions can be explained in terms of the successive reaction mechanism (e.g., $Br^- \rightleftharpoons Br^-(H_2O) \rightleftharpoons Br^-(H_2O)_2 \rightleftharpoons Br^-(H_2O)_3 \rightleftharpoons Br^-(H_2O)_4$). In addition, measurements of spin−lattice relaxation times have shown that the rate of rotational diffusion of water molecules is considerably slowed by the hydration of the ions.

Experimental Section

Materials. n-$(C_4H_9)_4N^+$ salts of bromide (Wako Pure Chemical Industries, Ltd.), iodide (Tokyo Kasei Kogyo Co. Ltd.), thiocyanate (Tokyo Kasei), perchlorate (Wako), and n-$(C_5H_{11})_4N^+$ chloride (Wako) were of the highest grade available. n-$(C_4H_9)_4N^+$ nitrate (Aldrich) was recrystallized from benzene to remove the chloride as an impurity. All the salts were dried at 50 °C under reduced pressure. NB-d$_5$ supplied by Isotec Inc. (99.5% atom D) was dried before use with a molecular sieve (4A; Wako).

Procedures. The alkylammonium salts of Cl^-, Br^-, I^-, NO_3^-, ClO_4^-, and SCN^- were dissolved in dry NB-d$_5$ (the anion

* Author to whom correspondence should be addressed. Fax: +81-78-803-5682. E-mail: osakai@kobe-u.ac.jp.
† Department of Chemistry, Faculty of Science.
‡ Department of Molecular Science, Graduate School of Science and Technology.

12022 *J. Phys. Chem. B, Vol. 104, No. 50, 2000*

Osakai et al.

concentration was 0−40 mM). The sample solutions containing water were prepared as follows: (1) add an aliquot of distilled water using a microsyringe to 25 mL of the NB-d$_5$ solution (or neat NB-d$_5$) in a glass bottle being placed in a water bath (25 ± 0.1 °C); (2) stir the solution for 10 min using a magnetic stirrer; (3) let stand for 20 min; (4) draw off an aliquot (0.5 mL) of the solution using a syringe, and transfer it to an NMR tube. Repeating this procedure (1)−(4) yielded the sample solutions containing various concentrations of water. During the preparation of sample solutions, the glass bottle was capped, except when necessary, to avoid water contamination from the atmosphere. Usually, degassing of the sample solutions was not performed, because no distinct influence of paramagnetic molecular oxygen was observed on the proton relaxation rate as well as the chemical shift.

Despite careful handling, it was not possible to evaluate the accurate concentration of water in the sample solution from the amount of addition, because some water contamination from the salts was inevitable. Accordingly, the water concentration was determined from the NMR signal of water protons in the following manner: The NB-d$_5$ solutions containing water (no salt) at various concentrations were prepared, and their water concentrations were determined in advance using a Karl Fischer coulometer (Kishida Chemicals CA-20). These solutions were then subjected to ^{1}H NMR measurements. Since the deuterated solvent contained a small but definite amount of protons, these protons as well as water protons gave some peaks in the NMR spectrum (see below). Against the integrated value of a peak due to the proton on the para position of the benzene ring, the "relative" integrated value of the peak for water protons was determined, which was found to be proportional to the water concentration determined by the Karl Fischer method. Using this linear calibration graph, the water concentration could be accurately determined for each sample containing salts.

The proton NMR spectra were measured at 400 MHz on a JEOL λ-400 spectrometer. An NMR tube with an outer diameter of 5 mm (Wilmad Glass Co., Inc.) was used, and the temperature was kept at 25 ± 0.1 °C. The chemical shifts of protons were measured using tetramethylsilane (TMS) as an internal reference.

Spin−lattice relaxation times, T_1, for water in NB-d$_5$ solutions were measured by the inversion−recovery method with the pulse sequence of $(180°−t−90°)_n$; the largest decay time t covered was longer than $3T_1$. In each sample solution, the free induction decay signals were accumulated 16 times, so that the Fourier-transformed spectra may attain a sufficient signal-to-noise ratio.

Under the extreme narrowing condition, which is realized here by the rapid molecular rotational motions, the spin−lattice relaxation rate ($1/T_1$) for the ^{1}H nucleus with the spin $I = 1/2$ is approximately expressed by[30]

$$\frac{1}{T_1} = \frac{3\gamma^4\hbar^2}{2r_{HH}^6}\tau_c \tag{1}$$

where γ is the proton gyromagnetic ratio, $\hbar$ is the Planck's constant (h) divided by 2π, r_{HH} is the intraproton distance of the water molecule, and τ_c is the rotational correlation time for the intramolecular ^{1}H−^{1}H axis. It is assumed here that $(1/T_1)$ consists of only intramolecular ^{1}H−^{1}H interaction. Because γ is related to the nuclear magnetic moment (μ) as $\hbar\gamma = \mu/$(angular momentum) $= \mu/(1/2) = 2\mu$, eq 1 can be rewritten as

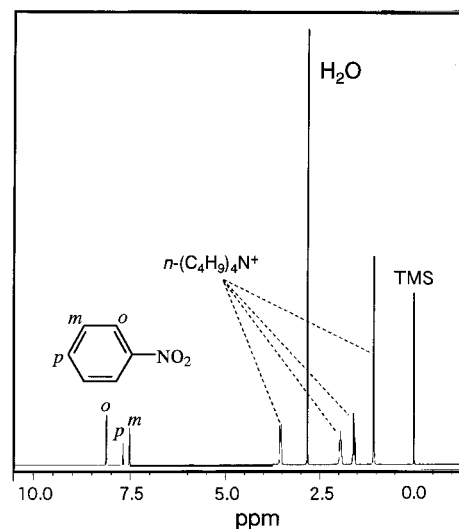$$\frac{1}{T_1} = \frac{3(2\mu)^4}{2r_{HH}^6\hbar^2}\tau_c \tag{2}$$

Figure 1. ^{1}H NMR spectrum at 400 MHz for a 20 mM Br$^-$ NB-d$_5$ solution containing 115 mM H$_2$O (25 °C).

Using values of r_{HH} (= 1.5143×10^{-8} cm)[31] and μ (= 1.4106×10^{-23} erg G^{-1}), one can obtain

$$\tau_c = \frac{1.41 \times 10^{-11}}{T_1}[s] \tag{3}$$

This relation enables us to obtain the value of τ_c from T_1 (in s).

Results and Discussion

Chemical Shifts. Figure 1 shows a typical NMR spectrum, which was obtained for a 20 mM Br$^-$ NB-d$_5$ solution containing 115 mM H$_2$O. As seen in the figure, the water protons always appeared as a singlet, because the exchange of water molecules associated and unassociated with the anion is very fast. Under these conditions, the chemical shift of water protons should change with the distribution of water molecules between some different states. The assignments of other signals are as follows: The signals round 1.0, 1.6, 2.0, and 3.5 ppm are due to the protons of n-(C$_4$H$_9$)$_4$N$^+$ used as the counterion of Br$^-$. The signals round 7.5, 7.7, and 8.1 ppm can be assigned, respectively, to m-, p-, and o-protons of the benzene ring of the solvent that remained undeuterated.

In Figure 2 the chemical shift of water protons, δ [ppm], is plotted against water concentration, [H$_2$O]$_{total}$, for six different anions. As seen in the figure, the chemical shift changed to lower magnetic fields in the order: ClO$_4^-$ < I$^-$ < SCN$^-$ < NO$_3^-$ < Br$^-$ < Cl$^-$, showing that the ion−water interaction becomes stronger in this order. This order is in harmony with that of the ionic radii[32] (nm): ClO$_4^-$ (0.236) > I$^-$ (0.216) > SCN$^-$ (0.195, 0.213) > Br$^-$ (0.195) > NO$_3^-$ (0.189) > Cl$^-$ (0.181). Also, the sequence of the chemical shifts agrees with that of the hydration numbers[10] in NB: ClO$_4^-$ (0.2) < I$^-$ (0.9) < SCN$^-$ (1.1) < NO$_3^-$ (1.7) < Br$^-$ (2.1) < Cl$^-$ (4.0). Furthermore, the sequence correlates closely with the $\Delta G_{tr}^{o,O\rightarrow W}$ values[13] of the anions (kJ mol^{-1}): ClO$_4^-$ (−7.9) > SCN$^-$ (−15.8) > I$^-$ (−18.4) > NO$_3^-$ (−25.2) > Br$^-$ (−27.8) > Cl$^-$ (−38.2). Thus, the chemical shifts of water protons show a good correlation with the hydrophilicity of the anions.

The chemical shifts for the "blank" solvent, i.e., NB-d$_5$ containing no ions, depended on water concentration to some extent, as shown by "Blank" in Figure 2. The low-field shift
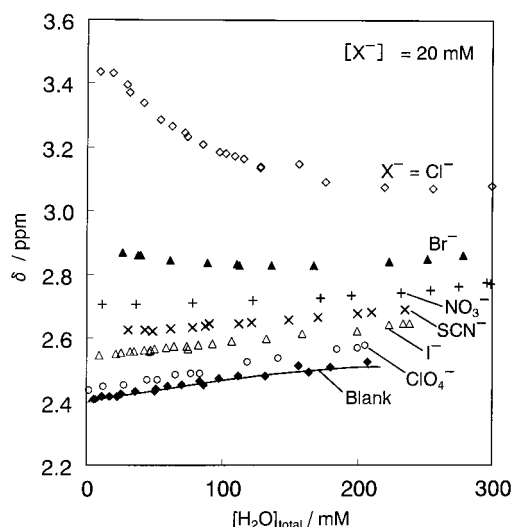
Selective Hydration of Anions in Nitrobenzene

J. Phys. Chem. B, Vol. 104, No. 50, 2000 **12023**

Figure 2. Plots of the chemical shifts of water protons against water concentration for various anions: $X^- = ClO_4^-$, I^-, SCN^-, NO_3^-, Br^-, and Cl^- at 20 mM in NB-d_5. The "Blank" represents the chemical shifts of water protons in the absence of the anions. The solid line represents the regression curve based on the monomer−dimer equilibrium (eq 4) for water.

Figure 3. Plots of the chemical shifts of water protons against water concentration for 10, 20, and 40 mM Br^- in NB-d_5. The solid lines show the best fit to the experimental data for the successive reaction mechanism (eq 10 with $m = 1-4$), while the dashed lines represent a set of theoretical curves based on the one-step reaction mechanism (eq 7).

with the water concentration can be analyzed on the basis of monomer−dimer equilibrium:[33]

$$2H_2O \rightleftharpoons (H_2O)_2 \qquad (4)$$

By assuming this equilibrium, the chemical shift of water protons is given by

$$\delta_{blank} = \frac{[H_2O]}{[H_2O]_{total}}\delta_{H_2O} + 2\frac{[(H_2O)_2]}{[H_2O]_{total}}\delta_{(H_2O)_2}$$

$$= \frac{[H_2O]}{[H_2O]_{total}}\delta_{H_2O} + 2\frac{K_s[H_2O]^2}{[H_2O]_{total}}\delta_{(H_2O)_2} \qquad (5)$$

where δ_{H_2O} and $\delta_{(H_2O)_2}$ are intrinsic chemical shifts of the monomer and dimer, respectively, and K_s is the monomer−dimer equilibrium constant for water:

$$K_s = \frac{[(H_2O)_2]}{[H_2O]^2} \qquad (6)$$

By using the reported value[23,33] of K_s (= 1.054 M^{-1}, at 25 °C), curve fitting with eq 5 was performed to obtain the regression curve shown in Figure 2. The intrinsic chemical shifts as fitting parameters were $\delta_{H_2O} = 2.40$ ppm and $\delta_{(H_2O)_2} = 2.87$ ppm, respectively. It should be noted that these values are very low compared with the chemical shift for bulk water ($\delta = 4.8$ ppm) or water clusters formed in certain organic solvents at low temperatures ($\delta = $ ca. 5 ppm); however, they are comparable to the chemical shifts for water monomers in hydrophobic solvents (1 ppm $< \delta <$ 3 ppm).[34] Thus, the observed higher-field signals for water protons allow us to suggest that water should hardly form any water clusters or hydrogen bond networks in such a hydrophobic solvent as NB.

As described above, the exchange processes of water molecules are too fast for the NMR to discriminate between their different states and only the averaged singlet lines for the protons of all different water molecules (free, autoassociated, and associated with the anions) have been gotten. The inter-
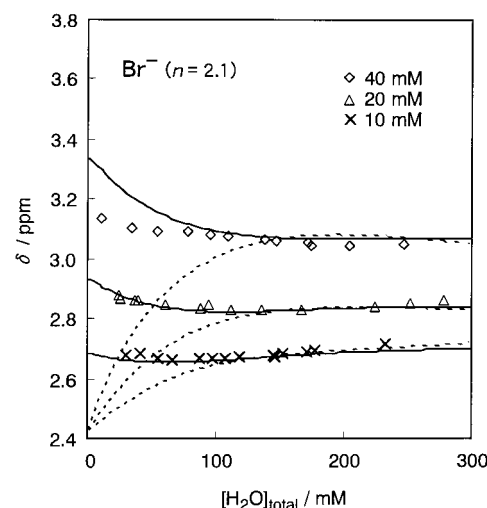
pretation of those spectra depends on the introduction of more or less speculative models whose validity can be verified indirectly. With a view to verifying the hydration models for the anions in NB, we have then examined the dependence of δ upon water- and ion-concentrations in detail. Figure 3 shows a typical example, in which the δ values for 10, 20, and 40 mM Br^- in NB-d_5 are plotted against the water concentration in the solvent. As seen in the figure, the chemical shift changed to lower fields with increasing ion concentration. A similar ion-concentration dependence of δ was also observed for all other anions, although the extent of the dependence differed from one anion to another.

The hydration number of Br^- has been reported to be $n = 2.1$ in NB.[10] Under the assumption that the dihydrated ion is formed by one step:
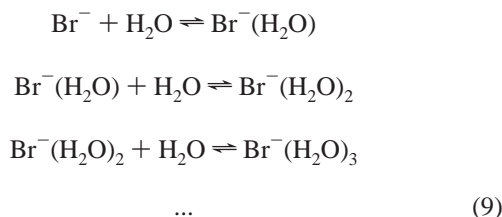
$$Br^- + 2(H_2O) \rightleftharpoons Br^-(H_2O)_2 \qquad (7)$$
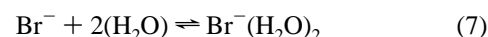
the chemical shift of water protons is given by (cf. eq 5)

$$\delta = \delta_{blank} + 2\frac{[Br^-(H_2O)_2]}{[H_2O]_{total}}\delta_{Br^-\cdot(H_2O)_2}$$

$$= \frac{[H_2O]}{[H_2O]_{total}}\delta_{H_2O} + 2\frac{K_s[H_2O]^2}{[H_2O]_{total}}\delta_{(H_2O)_2} +$$

$$2\frac{K_{one-step}[Br^-][H_2O]^2}{[H_2O]_{total}}\delta_{Br^-\cdot(H_2O)_2} \qquad (8)$$

where $\delta_{Br^-\cdot(H_2O)_2}$ is the intrinsic chemical shift for the dihydrated ion, $K_{one-step}$ the equilibrium constant of the hydration reaction (eq 7). However, the curve fitting with eq 8 was unsuccessful. The dashed lines in Figure 3 represent a set of theoretical curves based on the one-step reaction mechanism. As seen, the δ values at higher water concentrations can be simulated, but the dependence in the lower concentration range is entirely different from the observed one.

As an alternative approach, we assume that Br^- is hydrated in a stepwise fashion:

$$Br^- + H_2O \rightleftharpoons Br^-(H_2O)$$

$$Br^-(H_2O) + H_2O \rightleftharpoons Br^-(H_2O)_2$$

$$Br^-(H_2O)_2 + H_2O \rightleftharpoons Br^-(H_2O)_3$$

$$... \qquad (9)$$

In general, one can write for X^- ion:

$$X^-(H_2O)_{m-1} + H_2O \rightleftharpoons X^-(H_2O)_m \ (m = 1, 2, 3, ...) \quad (10)$$
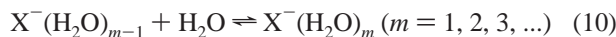
Such a successive reaction mechanism was previously employed by Ito et al.[23] to explain the chemical shift of water for the hydration of I^- in NB. On the basis of this mechanism, the observed chemical shift of water protons should be given by

$$\delta = \delta_{blank} + \frac{[X^-(H_2O)]}{[H_2O]_{total}}\delta_1 + 2\frac{[X^-(H_2O)_2]}{[H_2O]_{total}}\delta_2 +$$

$$3\frac{[X^-(H_2O)_3]}{[H_2O]_{total}}\delta_3 + ... + m\frac{[X^-(H_2O)_m]}{[H_2O]_{total}}\delta_m + ...$$

$$= \frac{[H_2O]}{[H_2O]_{total}}\delta_{H_2O} + 2\frac{K_s[H_2O]^2}{[H_2O]_{total}}\delta_{(H_2O)_2} + \frac{K_1[X^-][H_2O]}{[H_2O]_{total}}\delta_1 +$$

$$2\frac{K_1K_2[X^-][H_2O]^2}{[H_2O]_{total}}\delta_2 + 3\frac{K_1K_2K_3[X^-][H_2O]^3}{[H_2O]_{total}}\delta_3 + ... +$$

$$m\frac{K_1K_2K_3 ... K_m[X^-][H_2O]^m}{[H_2O]_{total}}\delta_m + ... \quad (11)$$

where δ_m ($m = 1, 2, 3, ...$) is the intrinsic chemical shift for the m-hydrated ion, and K_m the successive formation constant of the m-hydrated ion, which is defined by

$$K_m = \frac{[X^-(H_2O)_m]}{[X^-(H_2O)_{m-1}][H_2O]} \ (m = 1, 2, 3, ...) \quad (12)$$

The terms in eq 11 are interdependent of each other, because each term involves the concentration of monomeric water, $[H_2O]$. However, it should be noted that the crucial parameters involved in those terms (δ_m, K_m, K_s, etc.) are independent of each other, probably in the studied concentration range. By using the values of K_m, the concentration of the nonhydrated ion is given by

$$[X^-] = [X^-]_{total}/\{1 + K_1[H_2O] + K_1K_2[H_2O]^2 +$$

$$K_1K_2K_3[H_2O]^3 + ... + (K_1K_2K_3 ... K_m)[H_2O]^m + ...\} \quad (13)$$

where $[X^-]_{total}$ is the total concentration of X^-.

The experimental data were fitted with eqs 11−13 by assuming $m = 1, 2, 3$, and 4 for Br^- which has an average hydration number of 2.1. First, eq 13 was used with the initial values of K_m to evaluate $[X^-]$ as a function of $[H_2O]$, and then an iterative calculation was carried out with eq 11 to minimize the standard deviation, $\sigma = [\sum(\delta_{calcd} - \delta_{obsd})^2/(N - 1)]^{1/2}$, where δ_{calcd} and δ_{obsd} are calculated and observed chemical shifts, respectively, and N is the number of data points. In this curve-fitting procedure, the values of K_m and δ_m were used as adjusting parameters. In Figure 3, a set of the best regression curves for Br^- are shown by solid lines. In contrast to the one-step reaction mechanism, the successive reaction mechanism could reproduce
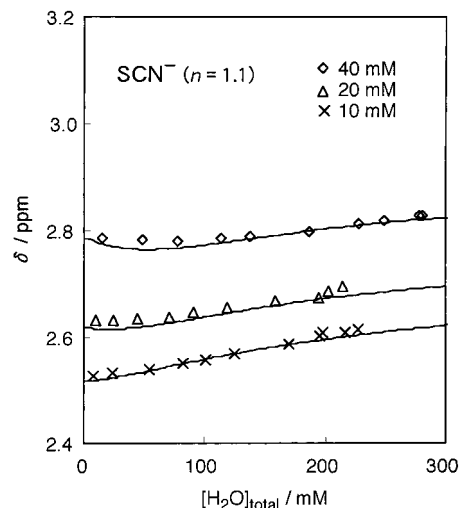

Figure 4. Plots of the chemical shifts of water protons against water concentration for 10, 20, and 40 mM SCN^- in NB-d5. Solid lines show the best fit to the experimental data for the successive reaction mechanism (eq 10 with $m = 1–3$).

the observed behaviors for δ reasonably well. It should be noted that in the successive reaction mechanism, the extrapolation of the fitting curves to zero water concentration gives different δ-values for the three different concentrations of Br^-. Although this may appear to be strange, it is understandable that a certain percentage of water should be associated with the anion, even at extremely low water concentrations (unless absolutely zero). Equation 12 with $m = 1$ (for lower water concentrations) clearly shows that the percentage of water molecules associated with the anion should be changed with the anion concentration.

For other anions with $n > 1.5$, i.e., Cl^- ($n = 4.0$) and NO_3^- ($n = 1.7$), curve fitting was also successful only with the successive reaction mechanism. However, in the case of the anions with $n < 1.5$, i.e., SCN^- ($n = 1.1$), I^- ($n = 0.9$), and ClO_4^- ($n = 0.2$), curve fitting was successful with both the successive and one-step reaction mechanisms. Nevertheless, since there would be no essential difference in hydration mechanism between the two anion groups, the successive reaction mechanism was adopted for the latter group (with $n < 1.5$) as well. Figure 4 shows the experimental chemical shifts for SCN^- together with their fitting curves based on the successive reaction mechanism as an example.

In Table 1 the values of K_m and δ_m obtained from the curve fittings are listed. It must be noted that these values were obtained as adjusting parameters and that not less than six parameters were used for each anion. Accordingly, these parameters could not be uniquely determined; a set of parameters obtained for each anion should be regarded as one of the best parameter sets that could give us a satisfactory result of the curve fitting. Although this prevents us from examining these parameters closely, there seem to be notable dependences of the parameters, especially for the monohydrated anions. The values of K_1 and δ_1 increase with the hydration number in NB. Because the hydration number shows a good correlation with the ionic radius (r) as described above, the K_1- and δ_1-values also correlate with r. This suggests that the ion−water interaction should be strengthened by an increase in the surface electric field which is inversely proportional to r.[13]

As seen in Table 1, the standard deviation was somewhat larger for NO_3^-, Br^-, and Cl^-. It is conceivable that these

Selective Hydration of Anions in Nitrobenzene

J. Phys. Chem. B, Vol. 104, No. 50, 2000 **12025**

TABLE 1: Values of K_m (M^{-1}) and δ_m (ppm) Obtained from the Curve Fittings Based on the Successive Reaction Mechanism (25 °C)

	ClO_4^-	I^-	SCN^-	NO_3^-	Br^-	Cl^-
K_1	3.7	6.5	7.4	7.4	7.5	13
K_2	1.9	3.0	3.5	4.9	6.5	11
K_3	1.6	3.0	3.5	3.4	6.5	11
K_4					7.0	10
K_5						10
K_6						9
δ_1	2.9	3.5	4.2	4.7	6.5	7.8
δ_2	2.7	3.5	3.1	3.5	3.2	4.0
δ_3	6.1	4.5	5.7	6.0	3.4	4.0
δ_4					5.2	4.0
δ_5						4.0
δ_6						4.6
σ^a	0.011	0.010	0.008	0.028	0.044	0.078
n^b	0.2	0.9	1.1	1.7	2.1	4.0
$\langle n \rangle^c$	0.6	1.2	1.3	1.6	2.6	5.3

^{a} Standard deviation, $\sigma = [\sum(\delta_{calcd} - \delta_{obsd})^2/(N - 1)]^{1/2}$, where δ_{calcd} and δ_{obsd} stand for the calculated and observed chemical shifts, respectively, and N is the number of data points. ^{b} Hydration number in NB.[10] ^{c} Average hydration number calculated using the K_m values.

comparatively hydrophilic anions are easier to form an ion pair with the countercation (R_4N^+) in NB: $X^- + R_4N^+ \rightleftharpoons X^- \cdot R_4N^+$. If this ion-pair formation is significant, it should affect the chemical shifts of water protons, because some or all of the water molecules associated with X^- would be released by the ion-pair formation. Therefore, we examined its effects in a typical case (i.e., $X^- = Br^-$; $R_4N^+ = n\text{-}(C_4H_9)_4N^+$) by assuming that the ion pair does not associate with any water molecules and that the ion-pair formation constant, K_{ip}, is independent of water concentration. The result showed that the regression curves in Figure 3 were improved to some extent (data not shown). However, the K_{ip} value as an adjusting parameter was 8.0 M^{-1}, indicating that the ion-pair formation is not very significant (the percentage of the ion pair is no more than 20% on the condition that $[Br^-]_{total} = [R_4N^+]_{total} \leq 40$ mM). Accordingly, to avoid useless complications, it has here been assumed that the anions do not form any ion pair in NB.

Finally, the present curve-fitting analyses have clearly shown that the selective hydration of anions in NB can be explained in terms of the successive reaction mechanism. In Figure 5, the distribution of the anions in several hydration states, calculated with the K_m-values in Table 1, are shown as a function of $[H_2O]_{total}$ for (A) SCN^- and (B) Br^-. For SCN^- with $n = 1.1$, the nonhydrated and monohydrated ions are most dominant at $[H_2O]_{total} \approx 180$ mM where NB containing 10 mM SCN^- is saturated with water at 25 °C. Such a relatively hydrophobic anion as SCN^- exists in the water-saturated NB mostly in the nonhydrated or monohydrated state, though there should be some highly hydrated ions. For this reason, the chemical shifts for ClO_4^-, I^-, and SCN^- could also be explained by the one-step reaction mechanism. On the other hand, as shown in Figure 5B, the Br^- ion with a higher hydration number ($n = 2.1$) exists in the water-saturated solvent (with $[H_2O]_{total} \approx 190$ mM) as the nonhydrated and differently hydrated states. This is the reason the chemical shifts for NO_3^-, Br^-, and Cl^- could not be reproduced by the one-step reaction mechanism assuming only one hydration state.

As also pointed out by Kusakabe,[8] the present results clearly show that the hydration number has no need to be an integer because it is always given as an averaged value over several species with different hydration numbers. Table 1 also shows
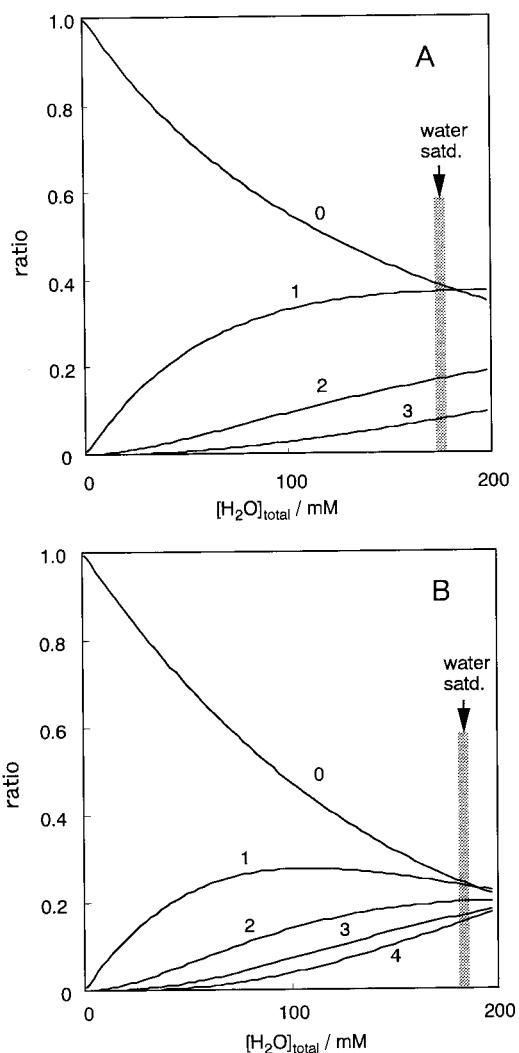

Figure 5. Distribution of the anions in several hydration states for (A) 10 mM SCN^- and (B) 10 mM Br^- as a function of water concentration: (0) nonhydrated; (1) monohydrated; (2) dihydrated; (3) trihydrated; and (4) tetrahydrated.

the "average" hydration numbers of the anions calculated by the following equation:

$$\langle n \rangle = \frac{\sum_m m([X^-(H_2O)_m]_{sat})}{[X^-]_{total}} \tag{14}$$

where $[X^-(H_2O)_m]_{sat}$ stands for the concentration of the m-hydrated ion in the water-saturated solvent. As seen in the table, the values of $\langle n \rangle$ are in accord with the values of n which were previously obtained by the Karl Fischer method.[10]

Rotational Correlation Times. Strictly speaking, the measured spin–lattice relaxation rate ($1/T_1$) consists of not only the intramolecular $^1H-^1H$ interaction (being given by the right-hand side of eq 1) but also "intermolecular" dipole–dipole interactions between the water proton and a nucleus of the hydrated anion. Although the exact evaluation of its contribution is impossible because of the lack of structural information for the hydrated anions in NB, a rough estimation[35] has shown that the contribution to $(1/T_1)$ is very small. Consequently, such outer-sphere relaxation contribution has been neglected to determine the rotational correlation times of water molecules on the basis of eq 1.

In the same manner as the chemical shifts, the rotational correlation times should be considered as the averaged values over several hydration states of water molecules. Figure 6 shows the plots of the rotational correlation time (τ_c) against $[H_2O]_{total}$ for several concentrations of Br^- (0, 10, 20, and 40 mM). As seen in the figure, the observed correlation times exhibited a clear dependence on $[H_2O]_{total}$ reflecting the concentration changes of the anions in several hydration states.

The τ_c-values for the blank solvent (i.e., for 0 mM Br^-) were only slightly dependent on $[H_2O]_{total}$ in the range of 2.8–2.9 ps, but simulated in a similar manner as the chemical shifts:

$$\tau_{c,blank} = \frac{[H_2O]}{[H_2O]_{total}}\tau_{H_2O} + 2\frac{[(H_2O)_2]}{[H_2O]_{total}}\tau_{(H_2O)_2}$$

$$= \frac{[H_2O]}{[H_2O]_{total}}\tau_{H_2O} + 2\frac{K_s[H_2O]^2}{[H_2O]_{total}}\tau_{(H_2O)_2} \quad (15)$$

where τ_{H_2O} and $\tau_{(H_2O)_2}$ are the intrinsic rotational correlation times for water monomer and dimer, respectively. The values of $\tau_{H_2O} = 2.8$ ps and $\tau_{(H_2O)_2} = 3.0$ ps were obtained as the fitting parameters. These values are somewhat larger than the τ-value (1.96 ps) for pure water,[36] in which hydrogen-bond networks are formed to retard the rotation of water molecules. However, upon considering the high viscosity of NB ($\eta = 1.795 \times 10^{-3}$ Pa·s at 25 °C; cf. $\eta = 0.890 \times 10^{-3}$ Pa·s for water),[37] the higher τ_c-values in NB seem to be reasonable for water monomer or dimer in NB.

As shown in Figure 6, the τ_c-values usually increased with the anion concentration. This dependence could also be expressed in terms of the successive reaction mechanism (eq 10). For this mechanism, the rotational correlation time of water molecules is generally given by

$$\tau_c = \tau_{c,blank} + \frac{[X^-(H_2O)]}{[H_2O]_{total}}\tau_1 + 2\frac{[X^-(H_2O)_2]}{[H_2O]_{total}}\tau_2 +$$

$$3\frac{[X^-(H_2O)_3]}{[H_2O]_{total}}\tau_3 + ... + m\frac{[X^-(H_2O)_m]}{[H_2O]_{total}}\tau_m + ...$$

$$= \frac{[H_2O]}{[H_2O]_{total}}\tau_{H_2O} + 2\frac{K_s[H_2O]^2}{[H_2O]_{total}}\tau_{(H_2O)_2} + \frac{K_1[X^-][H_2O]}{[H_2O]_{total}}\tau_1 +$$

$$2\frac{K_1K_2[X^-][H_2O]^2}{[H_2O]_{total}}\tau_2 + 3\frac{K_1K_2K_3[X^-][H_2O]^3}{[H_2O]_{total}}\tau_3 + ... +$$

$$m\frac{K_1K_2K_3 ... K_m[X^-][H_2O]^m}{[H_2O]_{total}}\tau_m + ... \quad (16)$$

where τ_m ($m = 1, 2, 3, ...$) is the intrinsic rotational correlation time of hydrated water molecules for the m-hydrated ion. Using the K_m-values obtained for the chemical shifts (Table 1), similar fitting analyses have been performed to obtain the τ_m-values as the fitting parameters. Thus, the present theoretical treatment enabled us to estimate the intrinsic contributions from hydrated water molecules in some different states.

As shown in Table 2, the τ_m-values are larger than ca. 3 ps for free water molecules, suggesting that the rotational motion of the hydrated water molecules should be restricted by the association with the anions. For the same reason as the intrinsic chemical shifts mentioned above, the obtained τ_m-values cannot be examined closely. Nevertheless, there is a notable tendency for τ_1 to increase with increasing the hydration number in NB
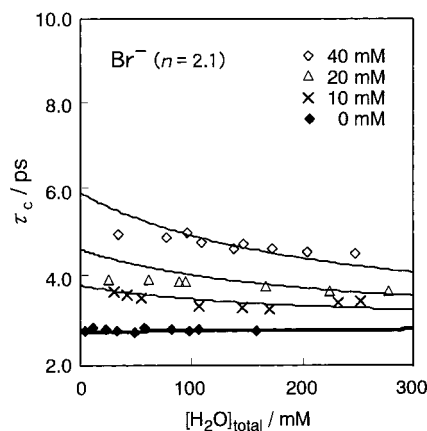

Figure 6. Plots of the rotational correlation times (τ_c) of water molecules against water concentration for several concentrations of Br^- in NB-d$_5$. The solid lines show the regression curves obtained by using eq 15 (for 0 mM Br^-) or eq 16 (for 10, 20, and 40 mM Br^-).

TABLE 2: Values of τ_m (ps) Obtained from the Curve Fittings Based on the Successive Reaction Mechanism (25 °C)

	ClO_4^-	I^-	SCN^-	NO_3^-	Br^-	Cl^-
τ_1	4.9	7.8	6.9	8.0	13.8	27
τ_2	7.1	13.5	13.7	4.0	6.6	7.3
τ_3	11.8	15.5	18.7	10.7	8.0	7.3
τ_4					7.3	7.3
τ_5						7.3
τ_6						7.3
σ^a	0.11	0.12	0.28	0.16	0.11	0.46

[a] Standard deviation, $\sigma = [\sum(\tau_{calcd} - \tau_{obsd})^2/(N - 1)]^{1/2}$, where τ_{calcd} and τ_{obsd} stand for the calculated and observed rotational correlation times, respectively, and N is the number of data points.

or the hydrophilicity of the anions. Regarding the relatively hydrophobic anions (ClO_4^-, I^-, and SCN^-), there is a marked tendency for τ_m to increase with m: $\tau_1 < \tau_2 < \tau_3$. However, this is not the case for other anions. It is probable that the τ_m-values reflect the structures of the hydrated anions which are still unknown at the present stage.

Concluding Remarks

^{1}H NMR spectroscopy was successfully employed to study the selective hydration of ions in water-immiscible organic solvents. The selective hydration of the inorganic anions can be explained well by the successive reaction mechanism. The rotational correlation time of free waters (monomeric or dimeric) in viscous NB is about 3 ps, which is considerably increased by the association with the anions. Measurements of the relaxation times for nuclei other than proton would give further information about the dynamic structures of hydrated ions.

References and Notes

(1) Rais, J.; Kyrš, M.; Pivoňková, M. *J. Inorg. Nucl. Chem.* **1968**, *30*, 611.

(2) Kawasaki, M.; Tôei, K.; Iwachido, T. *Chem. Lett.* **1972**, 417.

(3) Iwachido, T.; Minami, M.; Kimura, M.; Sadakane, A.; Kawasaki, M.; Tôei, K. *Bull. Chem. Soc. Jpn.* **1980**, *53*, 703.

(4) Yamamoto, Y.; Tarumoto, T.; Tarui, T. *Bull. Chem. Soc. Jpn.* **1973**, *46*, 1466.

(5) Kenjo, T.; Diamond, R. M. *J. Phys. Chem.* **1972**, *76*, 2454.

(6) Kenjo, T.; Diamond, R. M. *J. Inorg. Nucl. Chem.* **1974**, *36*, 183.

(7) Kusakabe, S.; Arai, M. *Bull. Chem. Soc. Jpn.* **1996**, *69*, 581.

(8) Kusakabe, S. *Solvent Extr. Res. Dev., Jpn.* **1997**, *4*, 147.

(9) Kusakabe, S. *Solvent Extr. Ion Exch.* **1997**, *15*, 219.

(10) Osakai, T.; Ogata, A.; Ebina, K. *J. Phys. Chem., B* **1997**, *101*, 8341.

(11) Marcus, Y. *Ion Solvation*; Wiley: Chichester, 1985; Chapter 7.

(12) Grigorieff, N.; Ceska, T. A.; Downing, K. H.; Baldwin, J. M.; Henderson, R. *J. Mol. Biol.* **1996**, *259*, 393.

(13) Osakai, T.; Ebina, K. *J. Phys. Chem., B* **1998**, *102*, 5691.

(14) Sánchez, C.; Leiva, E.; Dassie, S. A.; Baruzzi, A. M. *Bull. Chem. Soc. Jpn.* **1998**, *71*, 549.

(15) Benjamin, I. *Science* **1993**, *261*, 1558.

(16) Benjamin, I. *Liquid−Liquid Interfaces, Theory and Methods*; Volkov, A. G., Deamer, D. W., Eds.; CRC Press: Boca Raton, FL, 1996; Chapter 9.

(17) Volkov, A. G.; Paula, S.; Deamer, D. W. *Bioelectrochem. Bioenerg.* **1997**, *42*, 153.

(18) Paula, S.; Volkov, A. G.; Deamer, D. W. *Biophys. J.* **1998**, *74*, 319.

(19) Chantooni, M. K., Jr.; Kolthoff, I. M. *J. Am. Chem. Soc.* **1967**, *89*, 1582.

(20) Benoit, R. L.; Lam, S. Y. *J. Am. Chem. Soc.* **1974**, *96*, 7385.

(21) Izutsu, K.; Sakura, S.; Fujinaga, T. *Bull. Chem. Soc. Jpn.* **1972**, *45*, 445.

(22) Symons, M. C. R.; Jackson, S. E. *J. Chem. Soc., Faraday Trans. 1* **1979**, *75*, 1919.

(23) Ito, K.; Iwamoto, E.; Yamamoto, Y. *Bull. Chem. Soc. Jpn.* **1983**, *56*, 2290.

(24) Cogley, D. R.; Butler, J. N.; Grunwald, E. *J. Phys. Chem.* **1971**, *75*, 1477.

(25) Symons, M. C. R.; Thomas, V. K. *J. Chem. Soc., Faraday Trans. 1* **1981**, *77*, 1891.

(26) Kuntz, I. D., Jr.; Cheng, C. J. *J. Am. Chem. Soc.* **1975**, *97*, 4852.

(27) Symons, M. C. R.; Shippey, T. A.; Rastogi, P. P. *J. Chem. Soc., Faraday Trans. 1* **1980**, *76*, 2251.

(28) Tarui, T. *J. Inorg. Nucl. Chem.* **1975**, *37*, 1213.

(29) Kudryavtsev, A. B.; Linert, W. *Physicochemical Applications of NMR*; World Scientific: Singapore, 1996.

(30) Farrar, T. C.; Becker, E. D. *Pulse and Fourier Transform NMR, Introduction to Theory and Methods*; Academic Press: New York, 1971; Chapter 4.

(31) Calculated by using the O−H bond length (0.09575 nm) and $\angle$HOH angle (104.51°) for the gas-phase molecule of water; these values are available in *CRC Handbook of Chemistry and Physics,* 80th ed.; Lide, D. R. Ed.; CRC Press: Boca Raton, 1999.

(32) Marcus, Y. *Ion Solvation*; Wiley: Chichester, 1985; p 47.

(33) Johnson, J. R.; Christian, S. D.; Affsprung, H. E. *J. Chem. Soc. (A)* **1967**, 1924.

(34) Nakahara, M.; Wakai, C. *Chem. Lett.* **1992**, 809.

(35) Regarding the mono-atomic anion (i.e., Cl⁻, Br⁻, or I⁻), the contribution of the nuclear spin has been evaluated by assuming that the hydrated anion is a "rigid" molecule. Under the extreme narrowing condition, the contribution of the "intramolecular" dipole−dipole interaction to $(1/T_1)$ is given by $(4/3)[\gamma_I{}^2\gamma_S{}^2\hbar^2 S(S + 1)/r_{HX}{}^6]\tau_c$, where γ_I is the gyromagnetic ratio of the nucleus probed (i.e., proton); γ_S and S are the "effective" gyromagnetic ratio (considering the relative abundance of the isotopes) and the spin for the nucleus of the anion, respectively, and r_{HX} is the distance between the two nuclei (see Abragam, A. *The Principles of Nuclear Magnetism*; Oxford University Press: Oxford, 1961; Chapter 8). By assuming $(r_{HX}/nm) = 0.21$ (Cl⁻), 0.23 (Br⁻), and 0.26 (I⁻), the contributions from the respective anions have been estimated to be 0.4%, 1.8%, and 1.2%. In practice, these percentages should be furthermore reduced, because they should depend on the proportion of hydrated water molecules to the total water molecules.

(36) Shimizu, A.; Taniguchi, Y. *Bull. Chem. Soc. Jpn.* **1991**, *64*, 221.

(37) Riddick, J. A.; Bunger, W. B. *Organic Solvents*; Wiley-Interscience: New York, 1970.